J Fluoresc (2009) 19:663–671
DOI 10.1007/s10895-008-0459-2

ORIGINAL PAPER

Fabrication and Spectroscopic Characterization of Langmuir-Blodgett Films with Luminescent Rare Earth Complexes of Long Chain Double Functional Ligands Mono-L Phthalate (L = Hexadecyl, Octadecyl and Eicosyl)

Bing Yan · Bing Xu

Received: 13 September 2008 / Accepted: 16 December 2008 / Published online: 7 January 2009

Abstract In this paper, some novel long chain amphiphillic monoester molecules were designed to afford double functions: film-formation ability and luminescent sensitization ability. Subsequently organized molecular films of rare earth complexes with these functional ligands formulated as ML2NO3 were fabricated by the Langmuir-Blodgett film (LB) technology, where RE denotes rare earth ions Eu3+, Tb3+ and Dy3+; L denotes the long chain carboxylic ligands monohexadecyl phthalate (16-Phth), monooctadecyl phthalate (18-Phth) and monoeicosyl phthalate (20-Phth). The average molecular area was obtained according to the π-A isotherms. The layer structure of the LB films was demonstrated by low-angle X-ray diffraction and the average layer spacing was determined from the Bragg equation. UV absorption intensity increases linearly with the number of LB films layers, which indicates that the LB films are homogeneously deposited. The fluorescence spectra of these LB films were quite different from those of their solid complexes. It reveals that the long chain ester ligands are suitable for the excited states of Tb3+ and Dy3+ in the LB films as well as in the solid complexes, but not match with the europium ion in the LB films.

Keywords Langmuir-Blodgett film · Lanthanide complex · Long chain phthalate monoester · Luminescent property · Spectroscopy

B. Yan (✉) · B. Xu
Department of Chemistry, Tongji University,
Shanghai 200092, People's Republic of China
e-mail: byan@tongji.edu.cn

B. Yan
State Key Lab of Coordiantion Chemistry, Nanjing University,
Nanjing 210093, People's Republic of China

Introduction

Langmuir-Blodgett (LB) films have special characteristics, such as high orientation, controlled thickness and controllable molecular array for efficient energy and electron transfer [1–4], which attracted more and more attention of scientists because of their potential application in various areas of the microelectronics. In the decade, many luminescent lanthanide complexes have been deposited as ordered ultrathin film by Langmuir-Blodgett technology and the luminescence properties have been investigated [5–8]. Fanucci and Talham prepared several metal phosphate LB films based upon solid-state lanthanide (III) phosphaonates by Y-type deposition procedure [9]. Osvaldo et al. [10] prepared the LB films of europium complexes exhibiting strong fluorescence emission. Huang et al. [11, 12] combined rare earth anions with some organic molecules with nonlinear optical properties and found that the rare earth complex anions not only optimize the formation of the multilayers but also enhance the nonlinear optical efficiency of the organic molecules. However, β-diketone was used as the organic ligands in the preparation of LB films and moreover, in order to improve the film-forming ability, some researchers combined with rare earth complex anion and other long chain film-forming material into complex systems [13–15]. In these functional LB film systems, the film formation function and luminescent sensitization function is separated and the amphiphilic long chain molecules only provide film-forming ability and can not behave as energy donor. Besides, little work was reported on the aromatic carboxylic acid derivatives although they can be readily modified to achieve some new functions [14, 15]. It can be predicted that the modified aromatic carboxylic acid derivatives may present double function of both luminescence and film-formation.

In our recent work, three long chain carboxylic ligands (i.e. monohexadecyl phthalate (16-Phth), monooctadecyl phthalate (18-Phth), and monoeicosyl phthalate (20-Phth)) were prepared and the photophysical properties for their lanthanide complexes (Eu^{3+}, Tb^{3+} and Dy^{3+}) (The chemical structure as shown in Scheme 1) were studied in details, which were reported in ref. [16]. The nine lanthanide complexes were transferred successfully onto hydrophilic quartz substrate, i.e. their corresponding LB film were fabricated. The results of various measurements showed that these LB films were well organized and had luminescence properties. The experimental results indicate that the system can be used for the preparation of ultrathin films with luminescent properties. The new type of LB films can be expected to have potential applications in the fields of sensors and photoelectrochemical devices.

Experimental section

Measurements

UV-visible spectra were recorded on an Agilent 8453 spectrometer. The fluorescence (excitation and emission) spectra were determined with Perkin-Elmer LS-55 spectrometer: excitation slit width = 10 nm, emission slit width = 5 nm. X-ray diffraction data were obtained on a Rigaku D/max-γB X-ray diffractometer.

Preparation of LB films

LB films of the complexes were prepared by dropping their chloroform solutions (1×10^{-4} mol/L) onto a pure subphase of deionized water. The solvent was allowed to evaporate for at least 30 min prior to compressing, then the surface pressure vs area per molecule isotherms were recorded. The prepared monolayer was transferred onto a substrate by the vertical depositing method in Z-type model at a speed of 10 mm/min. The films were transferred onto substrates at a surface pressure of 20 mN/m for the Ln-16-Phth, 30 mN/m for the Ln-18-Phth and 40 mN/m for the Ln-20-Phth respectively. The transfer ratios of the films were around unity. The substrate for the emission measurements was a nonfluorescent quartz plate (10×30 mm). It was cleaned with sulfuric acid, dipped into 10% hydrogen peroxide solution and then rinsed with water.

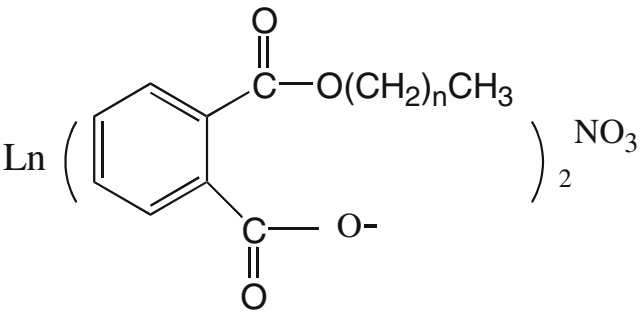

Scheme 1 Chemical formula of lanthanide complex with long chain carboxylic ester (n=15, 17, 19)

Results and discussion

π-A isotherms of monolayers

The π-A isotherms are shown in Fig. 1a–c and the related data are listed in Table 1. In Fig. 1a, the slope of the three curves is large and monotonously smooth without any noticeable phase transitions, which is related to LE and LC phases. The collapse pressure appears at about 27 mN/m, 30 mN/m, 27 mN/m in the π-A isotherm of Tb(16-Phth)$_2$NO$_3$, Dy(16-Phth)$_2$NO$_3$ and Eu(16-Phth)$_2$NO$_3$, respectively and the molecular areas obtained by extrapolating the steeply rising part of the curve to zero surface pressure are approximately 0.56 nm^2, 0.55 nm^2 and 0.57 nm^2, respectively for corresponding complexes. The exactly similar molecular structures conform to the similar shapes of the π-A isotherms, except for the small difference of the molecular areas which due to the difference of the three central ions of the rare earth complexes. In Fig. 1b, we can observe that the π-A isotherm of Tb(18-Phth)$_2$NO$_3$, Dy(18-Phth)$_2$NO$_3$ and Eu(18-Phth)$_2$NO$_3$ correspond to liquid expanded state of the lipid at the gas–water interface, the plateaus are about at 46 mN/m, 44 mN/m, 40 mN/m, respetively and the molecular areas are approximately 0.52 nm^2, 0.51 nm^2 and 0.53 nm^2, respectively. In Fig. 1c, the π-A isotherms of 20-Phth coordinated with the Tb^{3+}, Dy^{3+} and Eu^{3+} ions also have plateaus appeared at about 53 mN/m, 59 mN/m and 55 mN/m, and the corresponding molecular areas are 0.51 nm^2, 0.50 nm^2 and 0.52 nm^2, respectively. The π-A isotherm Eu(20-Phth)$_2$NO$_3$ and Tb (20-Phth)$_2$NO$_3$ present typical phase transition from gas state directly to solid state with the liquid phase absent while Dy(20-Phth)$_2$NO$_3$ has not any noticeable phase transitions [16]. The film-formation ability was greatly affected by the length of substituted alcohol chains. On one hand, the collapse pressure is increased with the increasing of length, suggesting that increasing length could increase the capacity of film forming. On the other hand, with the increasing length, the isotherm shifts towards a smaller area/per molecule, it can be assumed that long amphiphilic complex molecules oriented at hydrophilic substrate at an angle θ with the hydrophobic terminals stretch out in void,

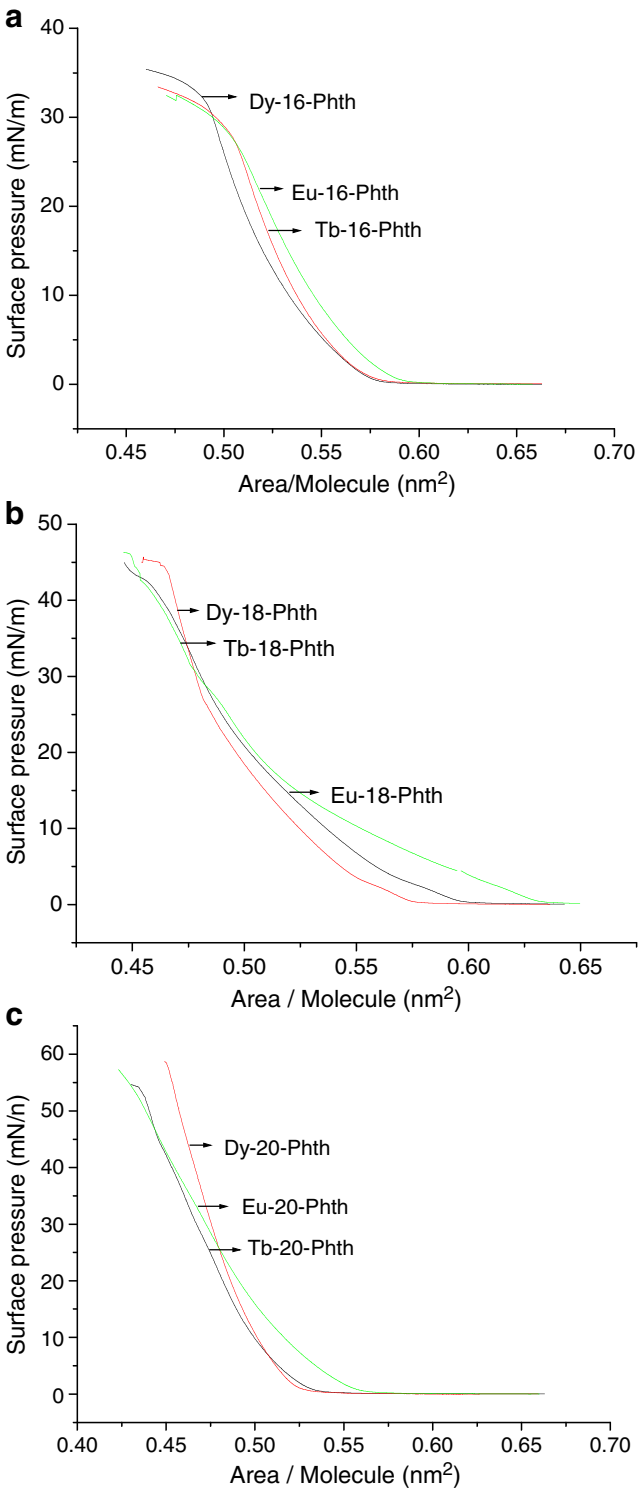

Fig. 1 π-A isotherms of lanthanide complexes LB films: **a** Ln-16-Phth; **b** Ln-18-Phth; **c** Ln-20-Phth (Ln = Eu, Dy and Tb)

the longer chain alkyls means the larger interaction, which make long chain molecules arrange more closely and be easily to stand perpendicular to substrate [17, 18]. Thus per molecule area has small value.

UV-Visible absorption spectra and low-angle X-ray diffraction

The UV-visible absorption spectra are shown in Fig. 2a–c. For the chloroform solution of the coordination compounds, the maximal peaks were located at 252 nm for Ln-16-Phth, 250 nm for Ln-18-Phth and 245 nm for Ln-20-Phth, respectively, which can be ascribed to the $\pi \rightarrow \pi^*$ transition of phenyl cycle with long-chain substituted groups. However, these peaks are all weak and not noticeable in their corresponding LB films. They appear at 230 nm, 233 nm and 235 nm for the 12 layers LB films of Ln-16-Phth, Ln-18-Phth and Ln-20-Phth, respectively. Besides, it is remarkable that a new strong absorption band occurs at 200 nm for the three LB films, which is probably caused by O→M transition [19]. These phenomena can be endorsed indeed to the film interactions and to the ordered arrangement of the molecules in the LB films. The lanthanide complexes in the solution are present as free single molecules, and the interactive forces among them can be neglected, but the complex molecules in the LB film are in an aggregate state with strong interactions. Figure 3 illustrates the relationship between absorption intensity of LB film of Dy-18-Phth and layer number at 200 nm. The linearity of the absorption intensity with respect to the number of layers was obtained, indicating that the film has a vertical homogeneity.

The low-angle X-ray diffractograms of 12-layered LB film of Tb-20-Phth LB films on quartz plates are shown in Fig. 4. It exhibits evident diffraction peaks at 0.738°, 2.214° and 4.584°, respectively, which are assigned to be (001), (003) and (006) Bragg diffraction, respectively, suggesting that the difference of growth of the molecular oritentation over LB films. This regular X-ray diffraction pattern points out that the LB film has a highly ordered layer structure. The average layer spacing of 9.57 Å is achieved according to the Bragg equation [20]. The other

Table 1 The collapse pressure and molecular area of lanthanide complex LB films from π-A isotherms

	Collapse pressure (mN /m)	Molecular area (nm2)	Compressibility
$Tb(16phth)_2NO_3$	27	0.56	perfect
$Dy(16phth)_2NO_3$	30	0.55	Perfect
$Eu(16phth)_2NO_3$	27	0.57	Perfect
$Tb(18phth)_2NO_3$	46	0.52	good
$Dy(18phth)_2NO_3$	44	0.51	good
$Eu(18phth)_2NO_3$	40	0.53	good
$Tb(20phth)_2NO_3$	53	0.51	perfect
$Dy(20phth)_2NO_3$	59	0.50	perfect
$Eu(20phth)_2NO_3$	55	0.52	perfect

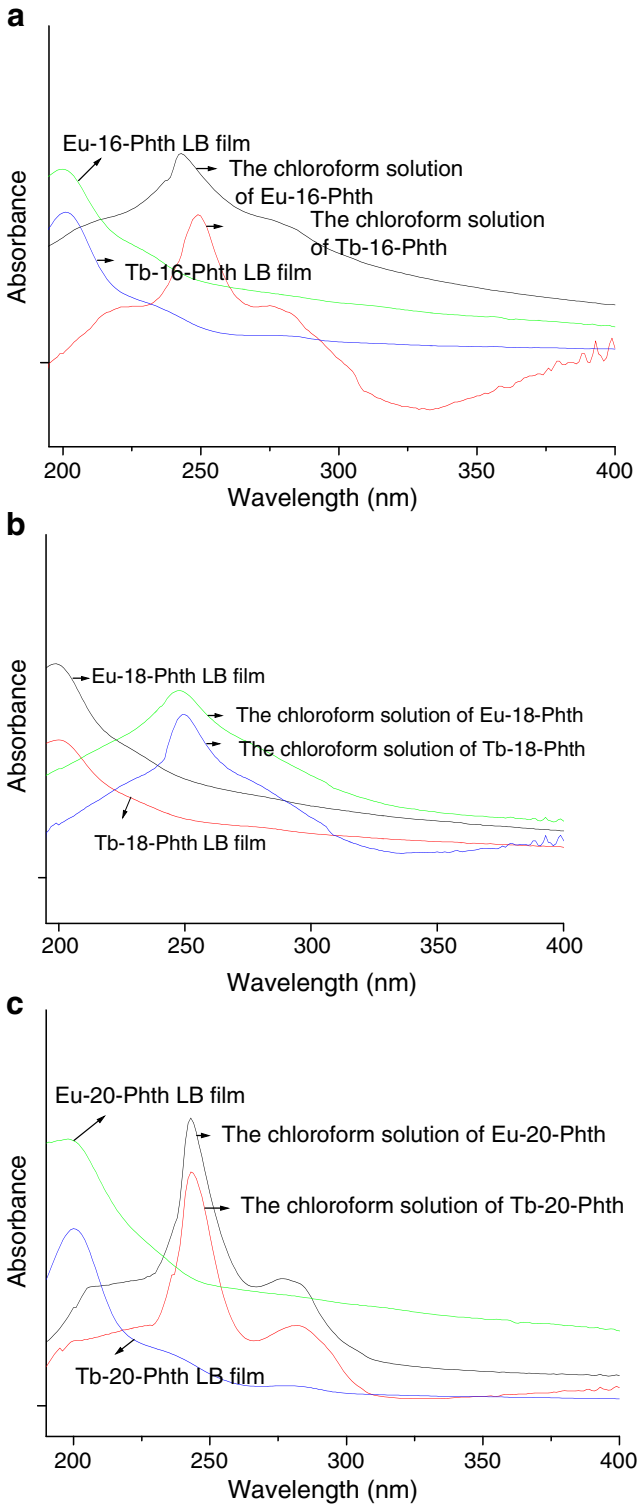

Fig. 2 Comparison of ultraviolet-visible absorption spectra of 12 layers lanthanide complexes LB films and chloroform solution: **a** Ln-16-Phth; **b** Ln-18-Phth; **c** Ln-20-Phth (Ln=Eu, Tb)

LB films of Tb complexes are also studied and their average layer spacing have been acquired, 8.2 Å for LB film of Tb-16-Phth and 8.8 Å for LB film Tb-18-Phth, which is increased with the increasing of the ligand' length.

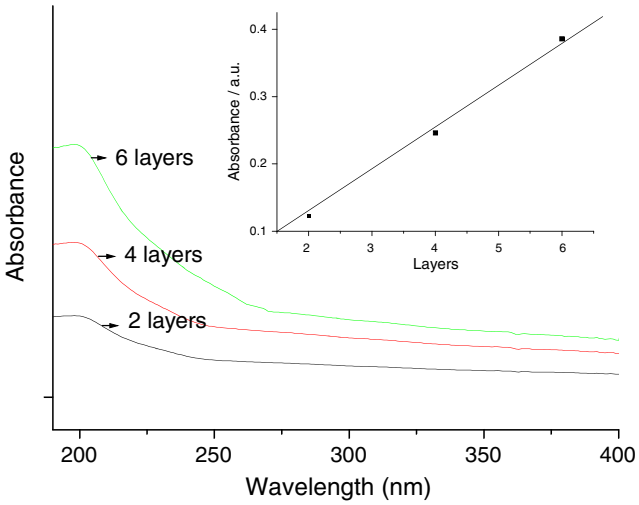

Fig. 3 Selected ultraviolet-visible spectra of 2, 4, 6 layers of LB film of Dy-18-Phth. The inset is the plot of absorbance at 200 nm against the number of layers

Luminescence properties

Figure 5a–c and Table 2 show the excitation spectra of LB film of Tb, Dy and Eu complexes with their powder complexes. The excitation bands for Tb complex LB films under the green emission of 545 nm exhibit a broad excitation bands and the maximum excitation peaks are located around 302 nm for LB film of Tb-16-Phth, 302 nm for LB film of Tb-18-Phth and 279 nm for LB film of Tb-20-Phth, respectively. The excitation spectrum of powder Tb complex shows a strong broad band with several small peaks, which may be due to the vibrational absorption of the ligands. The maximum excitation wavelengths locate at 351 nm for Tb-16-Phth powder complex, 352 nm for Tb-18-Phth powder complex and 326 nm for Tb-20-Phth powder complex. The broad band in the monolayer

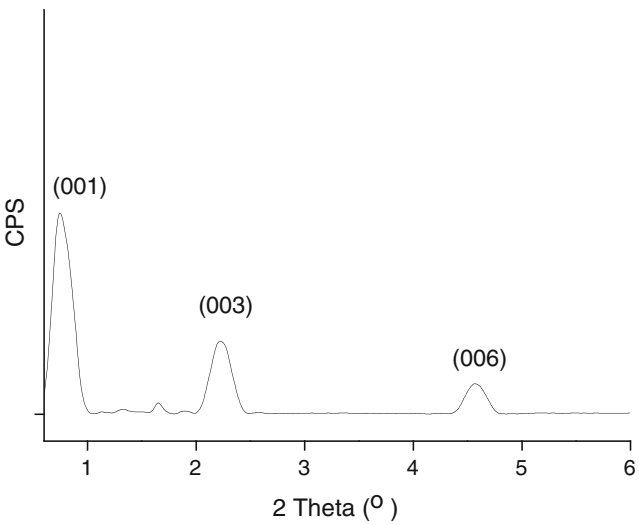

Fig. 4 Low-angle X-ray diffraction of 12 layers LB film of Tb-20-Phth

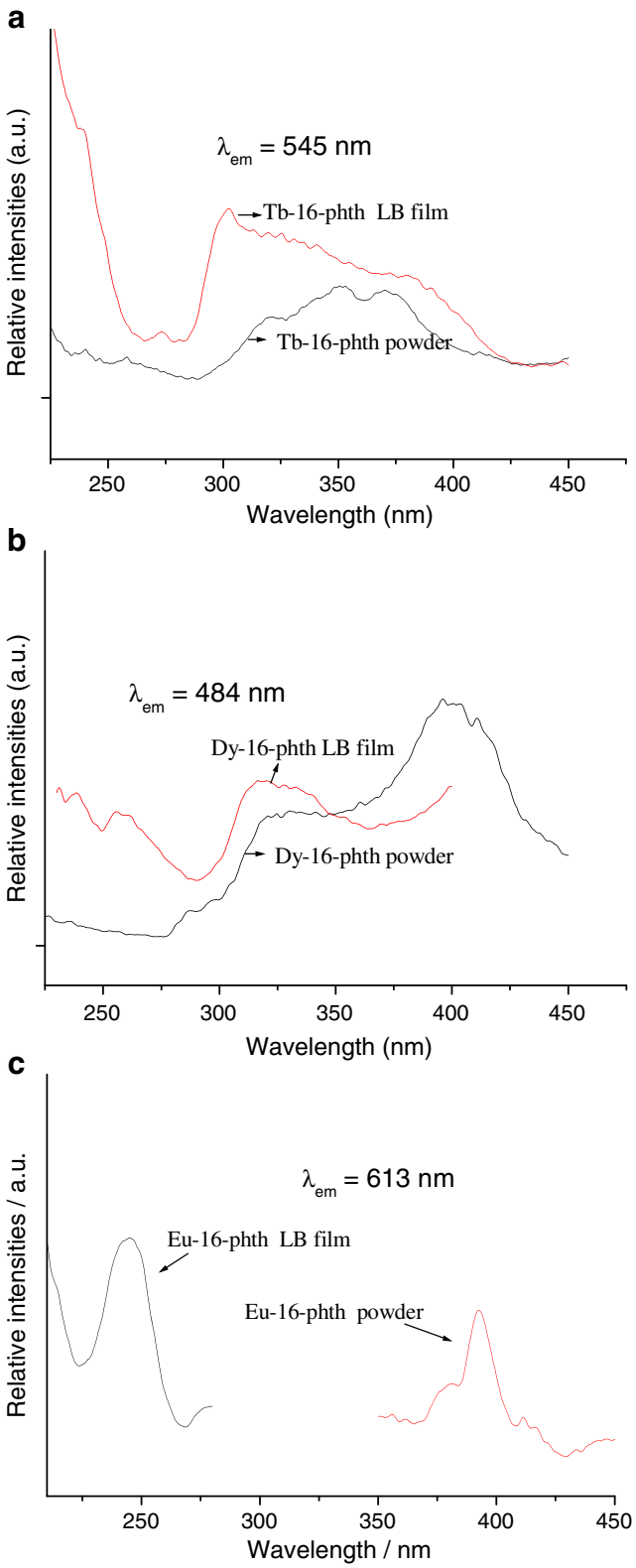

Fig. 5 Excitation spectra of Ln-16-Phth complex powders and Ln-16-Phth LB film: **a** Tb-16-Phth; **b** Dy-16-Phth; **c** Eu-16-Phth

assembly is shifted to shorter wavelength and broadened in comparison with that of the powder complex. The excitation bands for Dy complex LB films under the blue emission of 484 nm present a broad excitation bands and the maximum excitation peaks are to be found around 319 nm for LB film of Dy-16-Phth, 301 nm for LB film of Dy-18-Phth and 289 nm for LB film of Dy-20-Phth, respectively. The excitation spectrum of Dy powder complex shows a different broad band with several peaks, which are characteristic absorptions of Dy^{3+}. The maximum excitation wavelengths locate at 400 nm for Dy-16-Phth powder complex, 334 nm for Dy-18-Phth powder complex and 289 nm for Dy-20-Phth powder complex, respectively, which have shift to lower energy region and is narrower compared with that of the complex LB films. It has been demonstrated that the excitation spectrum of Tb, Dy complexes LB films and their powder complexes are dominated by a broad peak centered at 280–350 nm in the long ultraviolet-visible region which are the characteristic absorption of the lanthanide complexes arising from the efficient transition based on the conjugated −C=O double bonds. The excitation spectra of LB films from Eu complex under the red emission of 613 nm show that they have effective absorption in narrow wavelength ultraviolet region of the range 200–300 nm,whose maximum excitation peaks are located around 245 nm for LB film of Eu-16-Phth, 242 nm for LB film of Eu-18-Phth and 243 nm for LB film of Eu-20-Phth, respectively, which are originated from the efficient transition based on the conjugated double bonds of the aromatic ligand while the excitation spectrum of Eu powder complexes have the maximum excitation wavelengths at 395 nm for Eu-16-Phth powder complex, 395 nm for Eu-18-Phth powder complex and 392 nm for Eu-20-Phth powder complex, individually. This may be resulted from the characteristic absorption of the conjugated −C=O double bonds of the lanthanide complexes with long chain substitution.

The emission spectra of LB film of Tb, Dy and Eu complexes with their corresponding complexes powder were shown in Fig. 6a–c and some related data are shown in Table 2. When the Tb-16-Phth LB film is excited under 301 nm, two characteristic fluorescence emission peaks of Tb^{3+} at around 487 nm and 544 nm were obtained, corresponding to $^5D_4 \rightarrow {}^7F_6$ (induced electric dipole transition) and $^5D_4 \rightarrow {}^7F_5$ (electric dipole transition) transitions respectively. Among these transitions, the $^5D_4 \rightarrow {}^7F_6$ located at 487 nm is the stronger. The spectrum of Tb-16-Phth powder complex also shows the two characteristic transitions of Tb^{3+} at 490 nm and 543 nm. However, the shapes of the spectra and the relative intensity ratios ($^5D_4 \rightarrow {}^7F_5/{}^5D_4 \rightarrow {}^7F_6$) are different. The Tb-16-Phth powder complex has bigger fluorescence ratio (0.77) than the LB film (0.40). When the Tb-18-Phth LB film is excited under 302 nm, the $^5D_4 \rightarrow {}^7F_6$ transition at 486 nm and

Table 2 Comparison of the luminescence characteristics of LB films and the complex powders

Complexes	λex/nm	λex/nm (intensity/a.u.)		Ratio
		$^5D_4 \rightarrow {}^7F_6$	$^5D_4 \rightarrow {}^7F_5$	
$Tb(16phth)_2NO_3$[a]	302	487(131)	544(52)	0.397
$Tb(16phth)_2NO_3$[b]	352	490(70)	543(54)	0.771
$Tb(18phth)_2NO_3$[a]	302	487(87)	544(52)	0.597
$Tb(18phth)_2NO_3$[b]	351	490(77)	543(84)	1.091
$Tb(20phth)_2NO_3$[a]	279	487(72)	544(48)	0.667
$Tb(20phth)_2NO_3$[b]	326	487(43)	543(36)	0.837
		$^4G_{9/2} \rightarrow {}^7H_{15/2}$	$^4G_{9/2} \rightarrow {}^7H_{13/2}$	
$Dy(16phth)_2NO_3$[a]	319	485(46)	564(28)	0.609
$Dy(16phth)_2NO_3$[b]	400	481(100)	572(47)	0.470
$Dy(18phth)_2NO_3$[a]	301	484(71)	562(82)	1.155
$Dy(18phth)_2NO_3$[b]	334	483(100)	573(87)	0.870
$Dy(20phth)_2NO_3$[a]	289	484(103)	560(43)	0.417
$Dy(20phth)_2NO_3$[b]	290	482(100)	572(35)	0.350
		$^5D_0 \rightarrow {}^7F_1$	$^5D_0 \rightarrow {}^7F_2$	
$Eu(16phth)_2NO_3$[a]	245	598		
$Eu(16phth)_2NO_3$[b]	395	590(30)	614(44)	
$Eu(18phth)_2NO_3$[a]	242	598		
$Eu(18phth)_2NO_3$[b]	395	590(40)	616(54)	
$Eu(20phth)_2NO_3$[a]	243	598		
$Eu(20phth)_2NO_3$[b]	392	590(58)	616(63)	

[a] LB film, [b] complex powder

$^5D_4 \rightarrow {}^7F_5$ transition at 544 nm are gained. The emission spectrum of Tb-18-Phth powder is nearly same except that the relative intensity ratio (1.09) is bigger than that of LB film (0.60). The Tb-20-Phth LB film consists of two band, corresponding to the transition $^5D_4 \rightarrow {}^7F_6$ (487 nm) and $^5D_4 \rightarrow {}^7F_5$ (544 nm) of Tb^{3+}. However, the emission transitions of the complex powder show some different, for example $^5D_4 \rightarrow {}^7F_6$ at 487 nm and $^5D_4 \rightarrow {}^7F_5$ at 543 nm, whose intensity rations (0.84) is also bigger than that of LB films (0.67). So we can conclude that the difference observed in emission position and emission intensities ration also depends closely on the aggregation state of the molecules and the related small changes of the structure. Moreover it reveals that the long chain esters ligand is suitable for the excitation of Tb^{3+} in the LB films.

Comparing with the two characteristic transitions of Dy-16-Phth powder (481 nm and 572 nm, corresponding to $^4G_{9/2} \rightarrow {}^7H_{15/2}$ and $^4G_{9/2} \rightarrow {}^7H_{13/2}$ transitions respectively), while the spectrum of Dy-16-Phth LB film appears differently. The $^4G_{9/2} \rightarrow {}^7H_{15/2}$ transition (blue emission) shifts to a higher wavelength and the $^4G_{9/2} \rightarrow {}^7H_{13/2}$ one (yellow emission) give a wide band from 530 nm to 650 nm with the maximum wavelength at 564 nm, The Y: B values of the solid powders and the LB films are 0.470 and 0.609, respectively. The spectrum shape also exists in the other two LB films of Dy-18-Phth LB and Dy-20-Phth. Both show a peak at 484 nm and a wide band with the maximum at 562 nm and 560 nm, respectively, quite different from their corresponding powder complexes. The Y: B values of the powder complexes and the LB films are 0.870 and 1.155 for Dy-18-Phth, 0.350 and 0.417 for Dy-20-Phth, respectively. Analyzing the experimental results in the emission spectra, we think that the reason for the difference of Y: B values could be explained in the following way: it is well known that the yellow emission of $^4G_{9/2} \rightarrow {}^7H_{13/2}$ of Dy^{3+} is hypersensitive, which is influenced strongly by the outside surroundings. The transition probability between energy levels might be changed when the environment of molecular structure varied, and the ordered packing of molecules in LB films contributes to the fluorescence emission.

The luminescence data show that the long chain phthalate monoester ligands can effectively transfer some energy to the Tb^{3+} and Dy^{3+} in the LB films. Rare earth ions show generally very small absorption coefficients in the visible and UV region, whose luminescence can be enhanced through the effective energy transfer from organic ligands [21]. In principle, for complexes in which light absorption is performed in ligand-centered or charge-transfer bands, the organic ligands with suitable triplet level may be used to sensitize the luminescence of the rare earth ions. Thus the luminescence intensity depends on the ligand absorption intensity, the ligand-to-cation energy transfer efficiency and luminescence efficiency of rare earth ion itself. Our experimental results reveal that the triplet position of the long chain phthalate monoester ligand is

suitable for those of the excited states of the luminescent Tb^{3+} and Dy^{3+} ion in the LB films as well as in the basic compound powders.

The emission spectra of LB films and powders of Eu complexes were also different. It is surprised that the

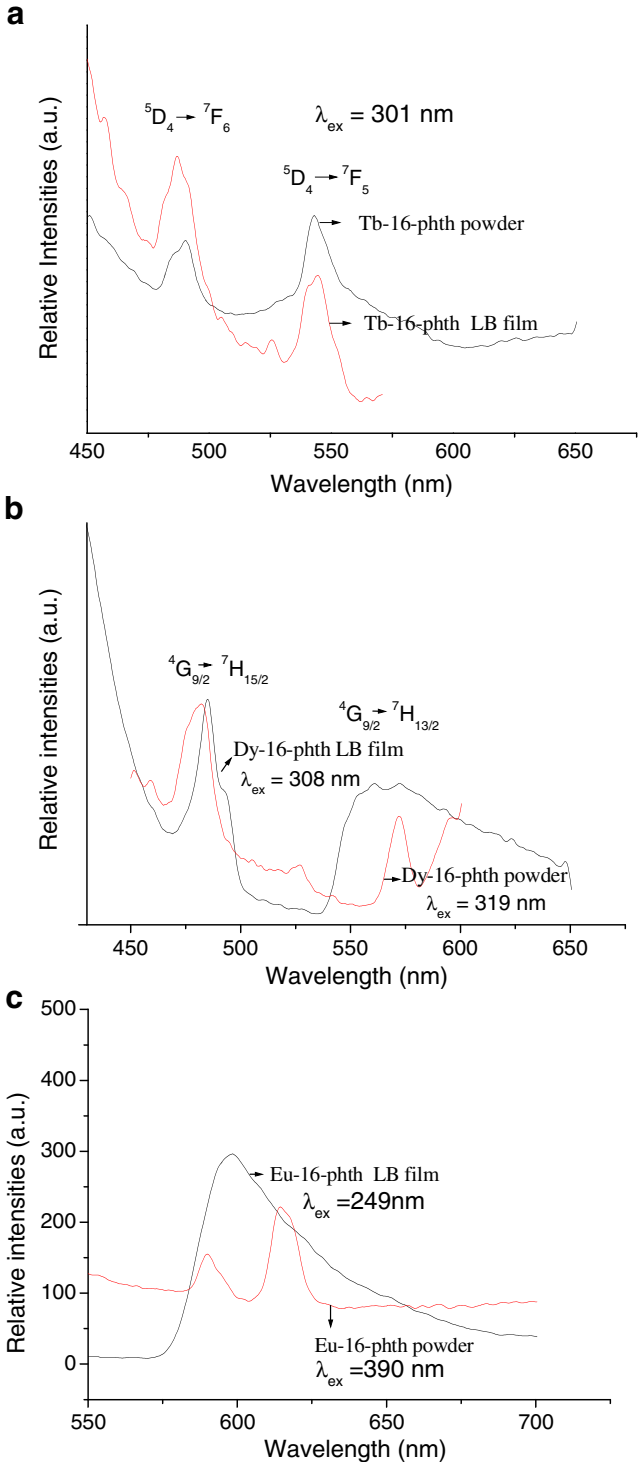

Fig. 6 Emission spectra of Ln-16-Phth complex powders and Ln-16-Phth LB film: **a** Tb-16-Phth; **b** Dy-16-Phth; **c** Eu-16-Phth

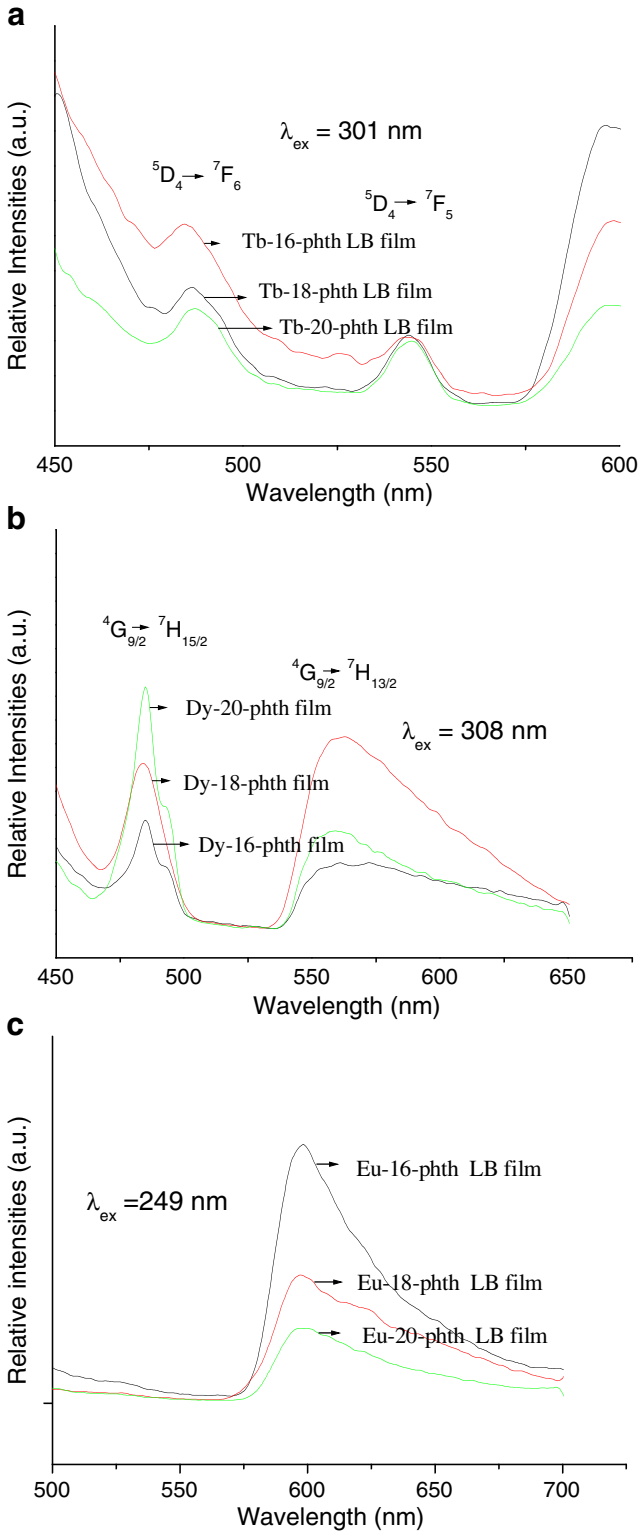

Fig. 7 Emission spectra spectra of lanthanide complex LB films with long chain esters: **a** Tb complex LB films; **b** Dy complex LB films; **c** Eu complex LB films

emission spectrum of Eu-16-Phth LB film under the excitation of 249 nm only have one peak from 570 nm to 640 nm with the maximum wavelength at 598 nm, while its corresponding powder complex under the excitation of 395 nm consist of two peaks, 594 nm and 614 nm, ascribed to the Eu^{3+} ion characteristic transitions of $^5D_0 \rightarrow {}^7F_1$ and $^5D_0 \rightarrow {}^7F_2$, respectively. The situation is same for another two Eu complexes systems. It well known that the evolution of Eu^{3+} fluorescence gives further insight on the rare earth environment [22]. The luminescence intensity depends on the ligand absorption intensity, the ligand-to-cation energy transfer efficiency and luminescence efficiency of rare earth ion itself. The fact that the excitation spectrum of the LB films of Eu complexes corresponds to free ligand absorption indicates that the pathway that results in the emission begins with excitation of a ligand π–π^* band of phenyl circle. Absorption of energy by the ground state singlet of carboxylic acid ligand results in an excited singlet state, which then goes through an intrasystem crossover to give the excited triplet state of the ligand, then energy is transferred to the rare earth ion and deactivated by fluorescence emission. The energy transfer distances of "Eu-ligand" were enlarged in the LB film packing of Eu complexes, resulting in transferring energy less effectively than that of Tb and Dy complexes LB film which are excited at −C=O band [23]. The change of molecular environment and order result in the difference of spectroscopy behaviors and the long carboxylic acid ester in LB films can not sensitize the europium ion effectively.

Figure 7a–c shows the selected emission spectra of LB films of Tb, Dy and Eu complexes with these three ligands. For the LB films of Tb, Dy and Eu complexes, their emission band keep unchanged with the increasing length of ligands, indicating that different chain lengths (16-Phth-18-Phth-20-Phth) have little influence on the emission band of these LB films.

Conclusions

Nine rare earth carboxylic ester complexes (ML_2NO_3) have been deposited on substrate by the Langmuir-Blodgett film (LB) technology. The mean molecule area is obtained and the layer structure of the LB films is demonstrated by low-angle X-ray diffraction. UV absorbance intensity increases linearly with the number of LB films layers, indicating that the LB films are homogeneously deposited. The fluorescence spectra of these LB films were quite different from those of their corresponding solid powders. It suggests that the long chain esters ligand can sensitize Tb^{3+} ion and Dy^{3+} ion in the LB films as well as in the compound powders, but not appropriate for the europium ion in the LB films.

Acknowledgements This word was supported by the National Natural Science Foundation of China (20671072).

References

1. Roberts GG (1990) Langmuir-Blodgett Films. Plenum
2. Lu WX, Guo WH, Zhou HL, He PS (2000) Component-controllable mixed monolayer and Langmuir-Blodgett films of Ru(dpphen)(3)(2+) and arachidic acid. Langmuir 16:5137 doi:10.1021/la991630l
3. Zasadzinski JA, Viswanathan R, Madsen L, Garnaes J, Schwartz DK (1994) Langmiur-Blodgett films. Science 263:1726 doi:10.1126/science.8134836
4. Schwartz K, Viswanathan R, Zasadzinski JA (1994) Examining Langmiur-Blodgett films with atomid-force microscopy. Science 263:1158 doi:10.1126/science.263.5150.1158
5. Zhang RJ, Liu HG, Yang KZ, Si ZK, Zhu GY, Zhang HW (1997) Fabrication and fluorescence characterization of the LB films of luminous rare earth complexes $Eu(TTA)_3Phen$ and $Sm(TTA)_3Phen$. Thin Solid Films 302:228 doi:10.1016/S0040-6090(96)09273-5
6. Zhang RJ, Yang KZ (1997) Fluorescence character of rare earth complex with high efficient green light in ordered molecular films. Langmuir 13:7141 doi:10.1021/la970156l
7. Huang YY, Yu A, Huang CH, Gan LB, Zhao XS, Lin Y, Zhang B (1999) Microcavity effect from a novel terbium complex Langmuir-Blodgett film. Adv Mater 11:627 doi:10.1002/(SICI)1521-4095(199906)11:8<627::AID-ADMA627>3.0.CO;2-A
8. Wang KZ, Huang CH, Xu GX, Zhao XS, Xia XH, Wu NZ, Xu LG, Li TK (1994) Optical properties of Langmuir-Blogdett film of hemicyanine containing the rare earth complex anion Dy $(BPMPHD)_2^-$. Thin Solid Films 252:139 doi:10.1016/0040-6090(94)90786-2
9. Fanucci GE, Talham DR (1999) Langmuir-Blodgett films based on known layered solids: Lanthanide(III) octadecylphosphonate LB films. Langmuir 15:3289 doi:10.1021/la980941d
10. Serra OA, Rosa ILV, Medeiros CL, Zaniquelli MED (1994) Luminescent properties of Eu^{3+} beta-dikentoneate complexes supported on Langmuir-Blodgett films. J Lumin 112:60
11. Huang CH, Wang KZ, Xu GX, Zhao XS, Xie XM, Xu LG, Li TK (1994) Molecular design and Langmuir-Blodgett film studies on a series of new nonlinear-optical rare earth complexes. Langmuir 10:3794 doi:10.1021/la00015a005
12. Huang CH, Wang KZ, Xu GX, Zhao XS, Xie XM, Xu Y, Liu YQ, Xu LG, Li TK (1995) Langmuir flim froming and 2nd harmonic generation properties of lanthanide complexes. J Phys Chem 99:14397 doi:10.1021/j100039a029
13. Zhou DJ, Huang CH, Wang KZ, Xu GX (1994) Langmuir-Blodgett-Flim and 2nd-harmonic generation of a europium hemicyanine complex $ME_2NC_6H_4CH{=}CHC_5H_4NC_{16}H_3{+}EU(NTA)_4^-$. Langmuir 10:1910 doi:10.1021/la00018a049
14. Zhang HJ, Li B, Ma JF, Ni JZ (1997) Luminescence properties of the Langmuir-Blodgett film of terbium(III) stearoylanthranilate. Thin Solid Films 310:274 doi:10.1016/S0040-6090(97)00391-X
15. Li B, Zhang HJ, Ma JF, Wang SB, Ni JZ (1996) Luminescence LB films of rare earth complexes with monooctadecyl phthalate. Chin Sci Bull 42:825 doi:10.1007/BF02882492
16. Yan B, Xu B (2005) Spectroscopic study on the photophysical properties of lanthanide complexes with long chain mono-docosyl phthalate. J Fluorescence 15:619 doi:10.1007/s10895-005-2835-5
17. Liu HG, Lan WZ, Yang KZ, Yun ZG, Zhang HW (1998) Studies on mixed europium complex octadecylamine monolayers with various molar ratios on an aqueous solution subphase surface. Thin Solid Films 323:235 doi:10.1016/S0040-6090(97)01037-7
18. Liang BJ, Yuan CW, Wei Y (1997) Determination of the molecular orientation of rare-earth bisphthalocyanine derivative Langmuir-Blodgett films by polarized ultraviolet-visible spectra. Spectrochim Acta [A] 53:531 doi:10.1016/S1386-1425(96)01821-5

19. Wang J, Wang HS, Liu FY, Fu LS, Zhang HJ (2003) LB films of 2-n-heptadecanoylbenzoic-rare earth and their luminescence properties. Synth Met 139:163 doi:10.1016/S0379-6779(03)00123-1
20. Koksharov YA, Bykov IV, Malakho AP, Polyakov SN, Khomutov GB, Bohr J (2002) Radicals as EPR probes of magnetization of gadolinium stearate Langmuir-Blodgett film. Mater Sci Eng C 22:201 doi:10.1016/S0928-4931(02)00181-9
21. Sabbtini N, Guardigli M, Lehn JM (1993) Luminescent lanthanide complexes as photochemical supramolecular devices. Coord Chem Rev 123:201 doi:10.1016/0010-8545(93)85056-A
22. Wang J, Wang HS, Fu HSLS, Liu FY, Zhang HJ (2002) Effective energy transfer and luminescence of LB films based on europium-substituted heteropolytungstate. Thin Solid Films 414:256 doi:10.1016/S0040-6090(02)00436-4
23. Wang QM, Yan B, Zhang XH (2005) Photophysical properties of novel lanthanide complexes with long chain mono-eicosyl *cis*-butene dicarboxylate. J Photochem Photobiol Chem 174:119 doi:10.1016/j.jphotochem.2005.02.016